*Romanian Reports in Physics, Vol. 63, Supplement, P. 1215–1235, 2011*

*Dedicated to Professor Marin Ivaşcu's 80th Anniversary*

# TRANSVERSE MOMENTUM-LONGITUDINAL MOMENTUM CORRELATIONS, THERMALIZATION AND HYDRODYNAMIC FLOW IN RELATIVISTIC NUCLEAR COLLISIONS

ALEXANDRU JIPA[1], CLAUDIAN GRIGORIE[2], CĂLIN BEŞLIU[1], ŞTEFANIA VELICA[1], MARIUS CĂLIN[1], TIBERIU EŞANU[1], IONEL LAZANU[1], VANIA COVLEA[1], DAN ARGINTARU[3], OANA RISTEA[1], CĂTĂLIN RISTEA[1], BOGDAN ILIESCU[1], AMELIA HORBUNIEV[4], SILVIU CIORANU[1], ADRIAN BÎRZU[1], FLORICA PARAGINĂ[1], SILVIU PARAGINĂ[1], DANIELA STOICA[1], VALERICA BABAN[1]

[1]Atomic and Nuclear Physics Department, Faculty of Physics, University of Bucharest, Romania
[2]National College "Alexandru Ioan Cuza" Corabia, Olt, Romania
[3]Physics Department, University of Civil Marine, Constanța, Romania
[4]National College "Ion Luca Caragiale" Bucharest, Romania
E-mail: jipa@brahms.fizica.unibuc.ro

*Received July 27, 2011*

*Abstract.* The transverse momentum-longitudinal momentum correlations are used to investigate the dynamics of the symmetric and asymmetric nucleus-nucleus collisions at 4.5 A GeV/c. The connections between different thermalization types and the hydrodynamic flow of the nuclear matter are discussed. The competition among different particle production mechanisms is investigated, also. Strong connections between the participant region geometry and nuclear matter flow are observed using the transverse momentum-longitudinal momentum correlations and the physical quantities given by global analysis for hydrodynamic flow.

*Key words*: relativistic nuclear collisions, thermalization, hydrodynamic flow, momentum correlations, particle production mechanisms.

## 1. INTRODUCTION

In a previous work we discussed on the possibility to use transverse momentum-longitudinal momentum correlations to evidence the competition among different particle mechanisms in nucleus-nucleus collisions at 4.5 A GeV/c [1]. In the present work we analyze the dependencies of the pionic temperatures on the linear correlation between transverse momentum and longitudinal momentum in the same collisions. These dependencies are discussed in the framework of the most important particle production mechanisms, namely: thermodynamic models

and hydrodynamic models [2-10]. Therefore, interesting parameters like: thermalization degree, flow angle, flow ratio etc. are discussed in comparison with the transverse momentum-longitudinal momentum correlations. Additional information on the competition between two particle production mechanisms using the hypothesis of the thermodynamic equilibrium in different manners (global equilibrium, in thermodynamic models, respectively, local equilibrium, in hydrodynamic models) can be obtained.

## 2. PIONIC TEMPERATURES AND TRANSVERSE MOMENTUM-LONGITUDINAL MOMENTUM CORRELATIONS

### 2.1. PIONIC TEMPERATURE RESULTS

The pionic temperatures for central and peripheral He-$A_T$ and C-$A_T$ collisions at 4.5 A GeV/c have been established from the transverse momentum distributions of the negative pions [11]. Each transverse momentum distribution has been fitted with the following relationship:

$$< p_T >= c_1 \mathrm{e}^{c_2 \frac{T}{T_0}}, \tag{1}$$

where the three parameters have the following values:

$$T_0 = 150 \text{ MeV}, \; c_1 = 382.2 \text{ MeV/c}, \; c_2 = -0.999 .$$

In the Table 1 are presented the pionic temperatures obtained in 8 nucleus-nucleus collisions at 4.5 A GeV/c, for peripheral collisions ($T$(0,0) triggering mode of the SKM 200 Spectrometer from the JINR Dubna (Russia) [1, 11]) and central collisions ($T$(2,0) triggering mode of the same spectrometer). Here, $N_{ev}$ is the number of events, $< p_T >$ represents the average transverse momentum, and $T$ is the pionic temperature for each collision.

The experimental results included in this table confirm that the pionic temperatures are higher in central collisions than in peripheral collisions for a given combination incident nucleus-target nucleus, at this energy per nucleon.

Another useful observation is related to the dependence of the pionic temperatures on the mass numbers of the colliding nuclei. For a given incident nucleus, the pionic temperatures increase with the increase of the mass number of the target nucleus. Reciprocally, for a given target nucleus, the pionic temperatures increase with the increase of the mass number of the incident nucleus. These dependencies reflect, once again, the importance of the collision geometry in relativistic nuclear collisions and what's happening in the participant region.

*Table 1*

Pionic temperatures for peripheral and central He-$A_T$ and C-$A_T$ collisions at 4.5 A GeV/c

| | Peripheral collisions $T$ (0,0) | | | Central collisions $T$ (2,0) | | |
|---|---|---|---|---|---|---|
| $A_P$ - $A_T$ | $N_{ev}$ | $< p_T >$ [MeV/c] | $T$ [MeV] | $N_{ev}$ | $< p_T >$ [MeV/c] | $T$ [MeV] |
| He – Li | 2975 | 242±1 | 68.4±0.9 | 1129 | 197±1 | 99.4±1.2 |
| He – C | 1901 | 240±1 | 69.6±0.9 | 911 | 195±1 | 100.7±1.1 |
| He – Ne | 834 | 234±2 | 73.3±1.4 | 507 | 189±2 | 105.7±1.7 |
| He – Al | 890 | 233±2 | 74.1±1.3 | 474 | 188±1 | 106.1±1.5 |
| He – Cu | 547 | 231±2 | 75.3±1.7 | 148 | 188±5 | 106.0±4.2 |
| He – Pb | 393 | 201±3 | 95.9±2.6 | 173 | 172±3 | 119.0±3.4 |
| C – C | 486 | 237±2 | 71.4±1.4 | 245 | 196±2 | 99.8±2.1 |
| C – Cu | 866 | 222±2 | 80.9±1.5 | 372 | 181±2 | 111.8±1.9 |

## 2.2. TRANSVERSE MOMENTUM-LONGITUDINAL MOMENTUM CORRELATIONS

Taking into account the necessity for obtaining the experimental information on the longitudinal-transverse momentum components we have considered the linear correlation between the two momentum components. In these conditions, to have equilibrium state the longitudinal momentum must decrease and transverse momentum must increase for all particles from a given event. If different collective particle production mechanisms – related to different equilibrium degrees – coexist, then it is possible to observe direct linear correlations between the two momentum components.

We introduced the linear correlation coefficient for the longitudinal and transverse momentum components for all charged particles, taking into account a previous conclusion related to the similar production mechanisms for negative pions and participants [see 1 and the references quoted]. The linear correlation coefficient is defined by the following relationship [12–17]:

$$r = \frac{\mathrm{cov}(\sigma)}{\sigma_{p_L}\sigma_{p_T}}, \tag{2}$$

where cov$(\sigma)$ is the covariance, $\sigma_{p_L}$ is the standard deviation for longitudinal momentum, and $\sigma_{p_T}$ is the standard deviation for transverse momentum, taking into account all n charged particles from an event. The covariance can be obtained using the following definition:

$$\mathrm{cov}(\sigma) = \frac{1}{n}\sum_{j=1}^{n}(p_{L_j} - < p_L >)(p_{T_j} - < p_T >), \tag{3}$$

with $< p_L > = \frac{1}{n}\sum_{k=1}^{n} p_{L_k}$ the average longitudinal momentum for the charged particles from an event, and $< p_T > = \frac{1}{n}\sum_{k=1}^{n} p_{T_k}$ the average transverse momentum for the charged particles from the same event.

Finally, we can write:

$$r = \frac{\sum_{j=1}^{n}(p_{L_j} - < p_L >)(p_{T_j} - < p_T >)}{\sqrt{\sum_{k=1}^{n}(p_{L_k} - < p_L >)^2 (p_{T_k} - < p_T >)^2}}. \tag{4}$$

For experimental values of the correlation coefficient the standard deviation can be estimated using the following relationship:

$$\sigma_r = \frac{1 - r^2}{n - 1}. \tag{5}$$

For analyzing the dependencies of the pionic temperatures on the linear correlation between the longitudinal momentum ($p_L$) and the transverse momentum ($p_T$) of the negative pions in the mentioned nucleus-nucleus collisions at 4.5 A GeV/c, 5 ranges of the linear correlation coefficient, $r$, have been considered, namely: $I_r^1 = [-1.0, -0.6]$; $I_r^2 = (-0.6, -0.2]$; $I_r^3 = (-0.2, 0.2)$; $I_r^4 = [0.2, 0.6)$ and $I_r^5 = [0.6, 1.0]$. Also, for each nucleus-nucleus collision, a selection of the events after the value of the linear correlation coefficient has been done. The pionic temperature has been calculated for each linear correlation coefficient range. The corresponding pionic temperatures have been noted as follows: $T_j$ for $r \in I_r^j$, where $j = 1,\ldots, 5$.

## 2.3. EXPERIMENTAL RESULTS

The calculations have been done for peripheral and central collisions. The experimental results obtained in peripheral nucleus-nucleus collisions at 4.5 A GeV/c are included in Table 2.

*Table 2*

Pionic temperatures in different linear correlation coefficient ranges
for peripheral nucleus-nucleus collisions at 4.5 A GeV/c

| $A_P - A_T$ | $T_1$ [MeV] | $T_2$ [MeV] | $T_3$ [MeV] | $T_4$ [MeV] | $T_5$ [MeV] |
|---|---|---|---|---|---|
| He – Li | 79.2±3.1 | 76.1±2.5 | 76.1±1.7 | 66.4±1.6 | 57.2±1.6 |
| He – C | 79.8±3.9 | 76.3±3.2 | 74.1±1.9 | 69.8±1.5 | 62.5±2.2 |
| He – Ne | 79.8±5.7 | 77.6±5.9 | 79.5±2.7 | 71.4±1.9 | 67.9±3.7 |
| He – Al | 79.0±5.6 | 78.0±5.5 | 78.0±2.9 | 71.4±2.0 | 71.0±1.8 |
| He – Cu | 91.0±6.9 | 89.2±6.7 | 83.7±3.4 | 73.4±2.3 | 65.7±2.0 |
| He – Pb | 117.2±7.1 | 116.9±7.0 | 116.0±6.3 | 102.5±3.7 | 84.8±3.8 |
| C – C | 72.7±5.7 | 71.2±5.6 | 69.9±4.2 | 68.9±2.2 | 67.5±2.3 |
| C – Cu | 89.7±4.7 | 88.4±4.3 | 87.0±4.0 | 87.1±3.0 | 71.4±2.3 |

Looking at the values included in Table 2 we can observe that, for a given collision, the pionic temperature decreases with the increase of the positive correlation and increases with the increase of the negative correlation. For each collision the pionic temperature associated with the first linear correlation coefficient range is greater than the pionic temperature associated with the fifth linear correlation coefficient range ($T_1 > T_5$). From Table 1 and Table 2 we obtain that the pionic temperature associated with the first linear correlation coefficient range, $T_1$, is greater than the global pionic temperature, $T$, from Table 1.

For central collisions, the experimental results are included in Table 3. Similar notations as in Table 2 are used. We can observe than the pionic temperatures obtained in central collisions are higher than those obtained in peripheral collisions, for all linear correlation coefficient ranges. A small increase of the pionic temperature with the negative correlation between the transverse momentum and longitudinal momentum can be suggested. For positive correlation between the two components of the momentum the pionic temperatures are almost the same, for a given collision. The dependencies of the pionic temperatures on the linear correlation coefficient range for He-Li collisions at 4.5 A GeV/c are presented in Fig. 1 (peripheral collisions) and Fig. 2 (central collisions).

*Table 3*

Pionic temperatures in different linear correlation coefficient ranges
for peripheral nucleus-nucleus collisions at 4.5 A GeV/c

| $A_P - A_T$ | $T_1$ [MeV] | $T_2$ [MeV] | $T_3$ [MeV] | $T_4$ [MeV] | $T_5$ [MeV] |
|---|---|---|---|---|---|
| He – Li | 98.6±3.8 | 93.8±3.7 | 98.3±3.5 | 101.0±2.5 | 99.9±1.7 |
| He – C | 100.9±4.1 | 102.0±3.1 | 95.8±2.7 | 99.5±2.2 | 103.4±2.0 |
| He – Ne | 114.5±7.9 | 108.4±6.3 | 110.3±3.8 | 100.7±3.4 | 104.1±2.6 |
| He – Al | 110.8±6.2 | 111.0±4.2 | 112.6±3.4 | 102.6±2.7 | 104.8±2.7 |
| He – Cu | 114.4±11.4 | 106.3±10.5 | 105.7±10.3 | 109.0±10.3 | 102.3±5.8 |
| He – Pb | 124.8±9.1 | 120.4±11.9 | 121.3±9.0 | 120.0±7.1 | 118.4±4.8 |
| C – C | 111.5±8.3 | 108.6±5.8 | 103.2±6.9 | 100.4±4.0 | 91.7±2.8 |
| C – Cu | 110.6±6.5 | 115.5±7.5 | 111.0±4.4 | 109.9±4.2 | 112.9±2.8 |

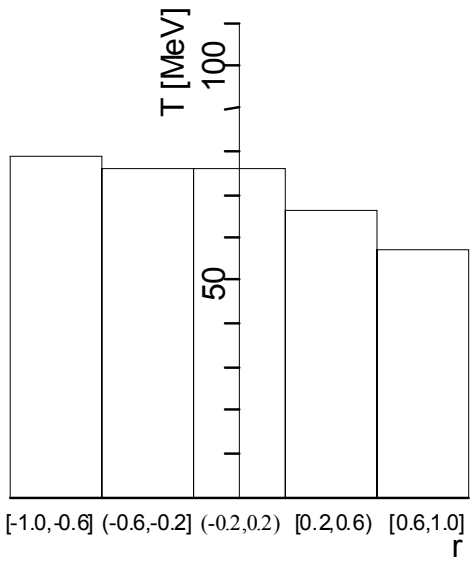


Fig.1 – Pionic temperature dependence on the linear correlation coefficient range in peripheral He-Li collisions at 4.5 A GeV/c.

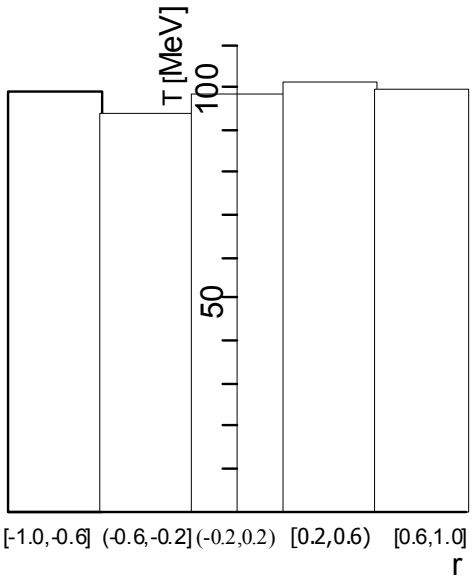


Fig. 2 – Pionic temperature dependence on the linear correlation coefficient range in central He-Li collisions at 4.5 A GeV/c.

The experimental results presented in the three tables suggest the dependence on the collision geometry, as well as the dependence on the correlation coefficient range for the two components of the momentum. The pionic temperature increases with the increase of the positive correlation between longitudinal momentum and transverse momentum. Therefore, the selection of the events with negative correlation between longitudinal momentum and transverse momentum can be used as method to evidence states of the nuclear matter with very high temperatures. The finding of such events could be a support to the hypothesis of the local equilibrium, as well as to the assumption of multiple particle sources in participant region.

## 3. SELECTION OF THE DYNAMIC PARAMETERS USING THE LINEAR CORRELATIONS GENERAL CONSIDERATIONS

In the investigation of the dynamics of the relativistic nuclear collisions different interesting parameters are used. These parameters take into account the influence of the collision geometry on the particle production mechanisms.

To select different interesting dynamic parameters we consider that the linear correlations between different physical quantities can be useful. Therefore, we use the general form of the relation (4), namely:

$$r = \frac{\sum_{i=1}^{n}(x_i - < x >)(y_i - < y >)}{\sqrt{\sum_{i=1}^{n}(x_i - < x >)^2 \sum_{i=1}^{n}(y_i - < y >)^2}}, \quad (6)$$

to obtain additional information on the collision dynamics and the competition among different mechanisms.

Taking into account that the greatest part of the current models uses the assumption of the thermodynamic equilibrium – global or local – we propose the study of some correlations which can help in the establishment of the type of equilibrium. We consider that interesting information on the collision dynamics can be obtained from the linear correlations between the following physical quantities: flow angle ($\theta_f$) and flow ratio ($F_{13}$) – noted by $r_{\theta_f F_{12}}$, flow angle ($\theta_f$) and thermalization degree $(R)$ – noted by $r_{\theta_f R}$, flow angle $(\theta_f)$ and charged particle multiplicity $(m)$ – noted by $r_{\theta_f m}$, flow ratio $(F_{13})$ and thermalization degree $(R)$ – noted by $r_{F_{13}R}$, flow ratio $(F_{13})$ and charged particle multiplicity $(m)$ – noted by $r_{F_{13}m}$.

## 3.1. EXPERIMENTAL RESULTS

We calculated the five correlation coefficients mentioned previously for the 8 nucleus-nucleus collisions at 4.5 A GeV/c considered in this work. As we mentioned, the central collisions offer more possibilities to obtain high temperatures and densities of the nuclear matter. Therefore, in Table 4 we present the results obtained in such collisions for these correlation coefficients.

*Table 4*

Values of the correlation coefficients for 8 central nucleus-nucleus collisions at 4.5 A GeV/c

| $A_P$-$A_T$ | $N_{ev}$ | $r_{\theta_f F_{13}}$ | $r_{\theta_f R}$ | $r_{F_{13}R}$ | $r_{\theta_f m}$ | $r_{F_{13}m}$ |
|---|---|---|---|---|---|---|
| He – Li | 1658 | -0.1839± 0.0005 | 0.6184± 0.0003 | -0.4987± 0.0004 | 0.0535± 0.0006 | -0.2370± 0.0005 |
| He – C | 1300 | -0.2092± 0.0007 | 0.6825± 0.0004 | -0.4875± 0.0005 | 0.0842± 0.0007 | -0.2975± 0.0007 |
| He – Ne | 569 | -0.2276± 0.0016 | 0.6470± 0.0010 | -0.5440± 0.0012 | -0.0051± 0.0017 | -0.2789± 0.0016 |
| He – Al | 632 | -0.1892± 0.0015 | 0.6073± 0.0010 | -0.5451± 0.0011 | -0.0350± 0.0015 | -0.3394± 0.0014 |
| He – Cu | 563 | -0.1862± 0.0017 | 0.6836± 0.0009 | -0.4929± 0.0013 | -0.1540± 0.0017 | -0.1845± 0.0017 |

*Table 4 (continued)*

| | | | | | | |
|---|---|---|---|---|---|---|
| He – Pb | 209 | -0.1519± 0.0047 | 0.6035± 0.0030 | -0.5354± 0.0034 | 0.0712± 0.0047 | -0.1910± 0.0046 |
| C – C | 472 | -0.1814± 0.0020 | 0.6740± 0.0011 | -0.5583± 0.0014 | 0.0156± 0.0021 | -0.4322± 0.0017 |
| C – Cu | 638 | -0.1850± 0.0015 | 0.5378± 0.0011 | -0.4960± 0.0011 | 0.0381± 0.0015 | -0.2746± 0.0014 |

The experimental results included in this table suggest the following behaviours:

– When the flow angle, $\theta_f$, increases, the flow ratio, $F_{13}$, decreases. This type of behaviour is normal (see Fig. 3, for example, where $\theta_f \to 90^0$, when $F_{13} \to 1$).

– The flow angle, $\theta_f$, increases with the increase of the thermalization degree, $R$, because the two physical quantities depend directly on the transverse momentum. It can be supposed that at the increase of the transverse momentum it can be expected an increase of the flow angle [Stocker], as well as of the thermalization degree.

– The thermalization degree increases when the flow ratio decreases and decreases when the flow ratio increases.

– Among the flow angle and multiplicities there are not a linear correlation.

– The flow ratio increases with the decrease of the multiplicity and it decreases with the increase of the multiplicity.

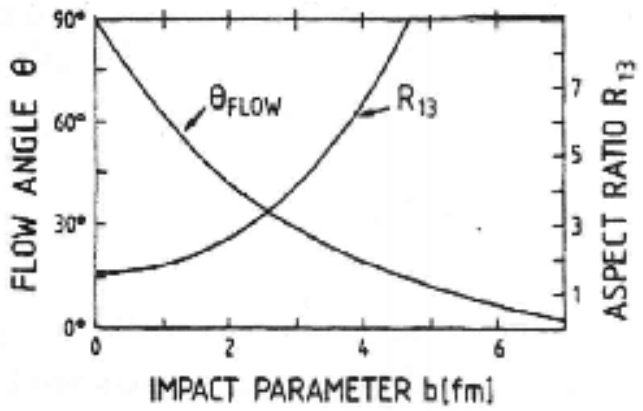


Fig. 3 – The dependencies of the flow angle and flow ratio on the impact parameter predicted by the hydrodynamic models [7].

*Table 5*

Correlation coefficients for random correlations for the same collisions as in Table 4

| $A_P$-$A_T$ | $N_{ev}$ | $r_{\theta f\text{-}rn}$ | $r_{Fc\text{-}rn}$ | $r_{R\text{-}rn}$ | $r_{m\text{-}rn}$ |
|---|---|---|---|---|---|
| He – Li | 1658 | 0.0132± 0.0006 | -0.0011± 0.0006 | 0.0103± 0.0006 | -0.0397± 0.0006 |
| He – C | 1300 | -0.0399± 0.0007 | 0.0531± 0.0007 | -0.0087± 0.0007 | 0.0445± 0.0007 |
| He – Ne | 569 | 0.0003± 0.0017 | 0.0736± 0.0017 | -0.0501± 0.0017 | -0.0038± 0.0017 |
| He – Al | 632 | 0.0003± 0.0015 | -0.0457± 0.0015 | -0.0324± 0.0015 | -0.0053± 0.0015 |
| He – Cu | 563 | -0.0346± 0.0017 | -0.0354± 0.0017 | 0.0498± 0.0017 | 0.0228± 0.0017 |
| He – Pb | 209 | -0.0192± 0.0048 | -0.1084± 0.0047 | -0.1098± 0.0047 | 0.0035± 0.0048 |
| C – C | 472 | -0.0074± 0.0023 | 0.0674± 0.0023 | 0.0007± 0.0021 | -0.0415± 0.0023 |
| C – Cu | 638 | -0.0011± 0.0015 | -0.0090± 0.0015 | -0.0209± 0.0015 | -0.0010± 0.0015 |

For increase the confidence in the results included in the Table 4 the linear correlation coefficients have been calculated for these parameters (flow angle, $\theta_f$, flow ratio, $F_c$, thermalization degree, $R$, multiplicity, $m$) and a random number, $rn$, from the range [0,1]. The results are included in Table 5. This analysis for the random correlations from this table indicated that the experimental correlations included in the Table 4 are not randomize, taking into account the values of the coefficients: $r_{\theta f\text{-}NRA}$, $r_{Fc\text{-}NRA}$, $r_{R\text{-}NRA}$ and $r_{m\text{-}NRA}$ are around 0.

## 4. ANALYSIS OF THE HYDRODYNAMIC FLOW OF THE NUCLEAR MATTER USING THE BIDIMENSIONAL NORMAL DISTRIBUTION

For obtaining additional information on the linear correlation between the longitudinal momentum, $p_L$, and transverse momentum, $p_T$, the two-dimensional normal distribution is introduced for the two components of the particle momentum (in this work, $\pi^-$) from a nuclear relativistic collision event. With this distribution one can obtain information about the dynamics of relativistic nuclear collisions and the nuclear matter flow.

This distribution is defined as [15–17]:

$$P(p_L, p_T) = \frac{1}{2\pi\sigma_{p_L}\sigma_{p_T}\sqrt{(1-r^2)}} \times$$

$$\times \exp\left\{-\frac{1}{2(1-r^2)}\left[\left(\frac{p_L - < p_L >}{\sigma_{p_L}}\right)^2 - 2r\frac{(p_L - < p_L >)(p_T - < p_T >)}{\sigma_{p_L}\sigma_{p_T}} + \right.\right. \tag{7}$$

$$\left.\left. + \left(\frac{p_T - < p_T >}{\sigma_{p_T}}\right)^2\right]\right\},$$

where: $< p_L > = \frac{1}{n}\sum_{i=1}^{n} p_{Li}$ is the mean value of the longitudinal momentum, $< p_T > = \frac{1}{n}\sum_{i=1}^{n} p_{Ti}$ is the mean value of the transverse momentum, $\sigma_{pL} = \left[\frac{1}{n}\sum_{i=1}^{n}(p_{Li} - < p_L >)^2\right]^{\frac{1}{2}}$ is the standard deviation of longitudinal momentum, $\sigma_{pT} = \left[\frac{1}{n}\sum_{i=1}^{n}(p_{Ti} - < p_T >)^2\right]^{\frac{1}{2}}$ is the standard deviation of transverse momentum, $r$ is the linear corelation coefficient between the longitudinal momentum ($p_L$) and transverse momentum ($p_T$) of a particle.

Using two-dimensional normal distribution for $p_L$ and $p_T$ components of the particle momentum in an event, we can write the equation of an ellipse as:

$$\left(\frac{p_L - < p_L >}{\sigma_{p_L}}\right)^2 - 2r\left(\frac{p_L - < p_L >}{\sigma_{p_L}}\right)\cdot\left(\frac{p_T - < p_T >}{\sigma_{p_T}}\right) + \left(\frac{p_T - < p_T >}{\sigma_{p_T}}\right)^2 = \tag{8}$$

$$= -2(1-r^2)\ln(1-\alpha),$$

where $\alpha$ is the probability that random vector ($p_L$, $p_T$) take values in the ellipse.

Ellipse obtained in the ($p_L$, $p_T$) plane confirm the ellipsoidal shape obtained by global analysis [1, 7, 18, 19] – where the authors propose to build a tensor using the particle momenta – and also confirm the ellipsoidal shape of a pionic source obtained by identical particle interferometry [20–22]. Using this equation we can calculate the $\alpha$ probability for different relativistic nuclear collisions.

For this ellipse we can define the angle between the large ellipse axis (1) and the incident beam direction through the relationship:

$$\xi = \frac{1}{2}\operatorname{arctg}\left[\frac{2r\sigma_{p_L}\sigma_{p_T}}{\sigma^2_{p_L} - \sigma^2_{p_T}}\right]. \tag{9}$$

Depending on the parameters $r$, $\sigma_{pL}$ and $\sigma_{pT}$, ellipse defined by equation (8) is represented in the ($p_L$, $p_T$) plan, as follows:

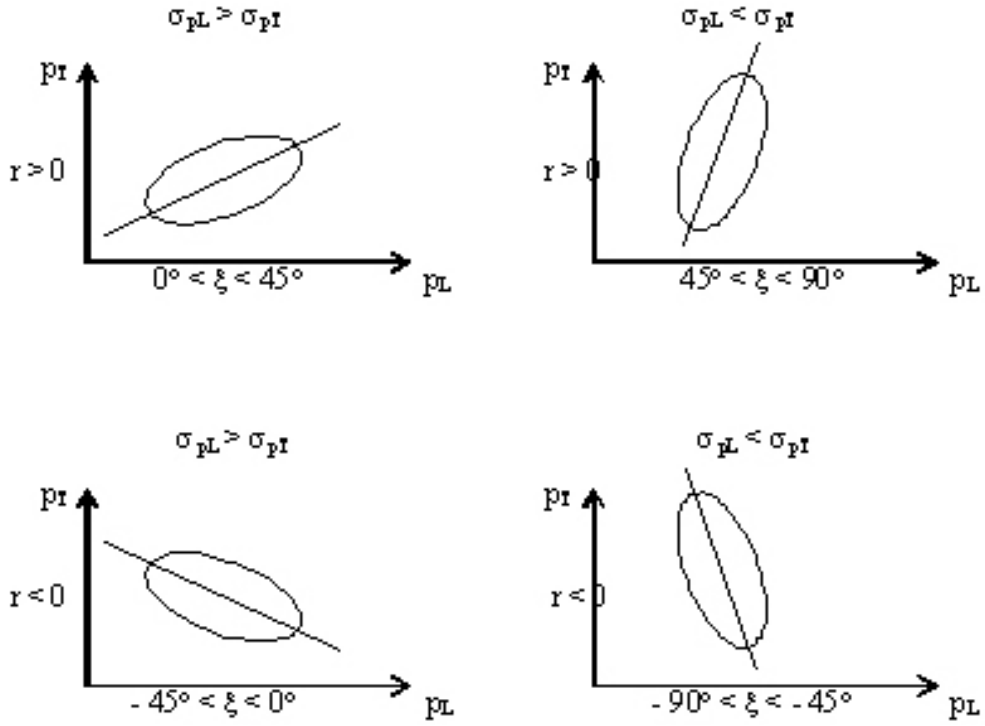


Fig. 4 – Different forms and orientations of the ellipse in the ($p_L$, $p_T$) plane.

We can make a connection between this angle – between the large axis of the ellipse (8) and incident beam direction – and the "thrust" angle – which is the most likely angle of the nuclear matter flow – and we can obtain informations about the nuclear matter flow. The experimental results obtained in relativistic nuclear collisions at 4.5 AGeV/c have confirmed this connection.

For a central He-Pb nuclear collision, the probability that the ($p_L$, $p_T$) vector to take values inside the ellipse (1) is $\alpha = 0.87 \pm 0.05$. The longitudinal and transverse momenta for negative pions produced in a central He-Pb collisions in the ($\langle p_L \rangle$, $\langle p_T \rangle$) plane, are presented in Fig. 5.

Using the formula (9) were determined both positive and negative angles $\xi$ for peripheral and central nuclear collisions and the average values of these angles, $\langle \xi^+ \rangle$ for positive angles and $\langle \xi^- \rangle$ for negative angles.

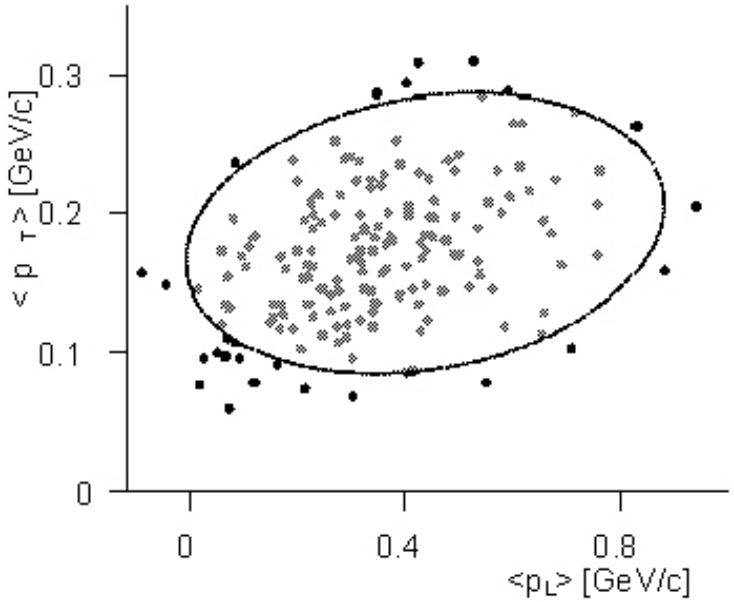


Fig. 5 – The longitudinal and transverse momenta for negative pions produced in a central He-Pb collisions in the ($<p_L>$, $<p_T>$) plane.

In Table 6 are presented the results for peripheral nuclear collisions, and in Table 7 are presented the data for central nuclear collisions. In these tables $N_{ev}$ is the total number of experimental events, $N_{ev}^{+}$ represents the number of events positively correlated (have the linear correlation coefficient $r \geq 0.0$), and $N_{ev}^{-}$ represents the number of events negatively correlated (have the linear correlation coefficient $r < 0.0$).

*Table 6*

The average values of the angles, for peripheral nuclear collisions
($<\xi^{+}>$ is for positive angles, and $<\xi^{-}>$ is for negative angles)

| $A_P - A_T$ | $N_{ev}$ | $N_{ev}^{+}$ | $N_{ev}^{-}$ | $<\xi^{+}>$ [°] | $<\xi^{-}>$ [°] |
|---|---|---|---|---|---|
| He – Li | 2975 | 1853 | 1122 | 1.99±0.05 | 1.04±0.04 |
| He – C | 1904 | 1364 | 540 | 1.67±0.09 | 1.29±0.17 |
| He – Ne | 834 | 629 | 205 | 1.55±0.10 | 1.10±0.18 |
| He – Al | 891 | 675 | 216 | 1.93±0.15 | 1.10±0.16 |
| He – Cu | 548 | 444 | 104 | 2.19±0.19 | 1.49±0.78 |
| He – Pb | 395 | 352 | 43 | 2.23±0.25 | 3.01±1.64 |
| C – C | 490 | 407 | 83 | 3.68±0.31 | 2.49±1.06 |
| C – Cu | 867 | 624 | 243 | 3.15±0.15 | 2.09±0.37 |

*Table 7*
The average values of the angles, for central nuclear collisions ($T(2,0)$)
($<\xi^+>$ is for positive angles, and $<\xi^->$ is for negative angles)

| $A_P - A_T$ | $N_{ev}$ | $N_{ev}^+$ | $N_{ev}^-$ | $<\xi^+>$ [°] | $<\xi^->$ [°] |
|---|---|---|---|---|---|
| He – Li | 1129 | 831 | 298 | 9.52±0.38 | 9.41±0.81 |
| He – C | 911 | 639 | 272 | 10.36±0.43 | 9.50±0.88 |
| He – Ne | 507 | 375 | 132 | 11.08±0.60 | 8.53±1.04 |
| He – Al | 474 | 330 | 144 | 10.37±0.69 | 9.58±1.22 |
| He – Cu | 148 | 102 | 46 | 17.39±1.51 | 16.78±3.30 |
| He – Pb | 173 | 123 | 50 | 15.69±1.49 | 8.63±1.74 |
| C – C | 245 | 167 | 78 | 9.16±0.63 | 10.79±1.81 |
| C – Cu | 372 | 266 | 106 | 8.51±0.41 | 8.47±1.21 |

From these tables, we see that the mean values of the angles increase with increasing the mass number of target nucleus for both peripheral and central collisions and the mean value for positive angles, $<\xi^+>$, is greater than the mean value for negative angles , $<\xi^->$ for any nuclear collision, regardless of the type of collision. Also, we notice that the mean values of the angles, $\xi^+$ and $\xi^-$, for central collisions are higher than for peripheral collisions. These mean angles obtained for the nuclear collisions at an incident beam momentum of 4.5 AGeV/c can be considered the most probable angles of flow for the nuclear matter, and there is a strong connection with the "thrust" angle obtained by global analysis.

Positive angle distributions for He-Li nuclear collision are shown in Fig. 6 and Fig. 7, respectively.

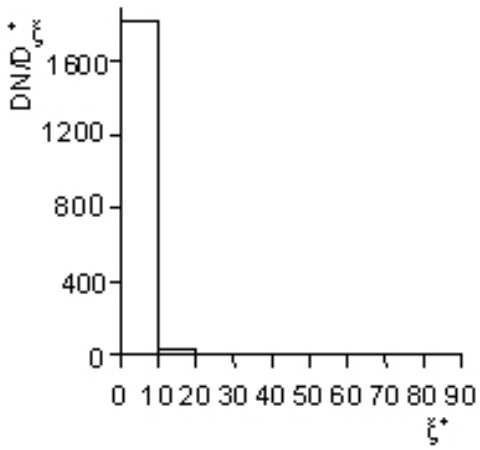


Fig. 6 – The $\xi^+$ angle distribution for peripheral He-Li nuclear collision.

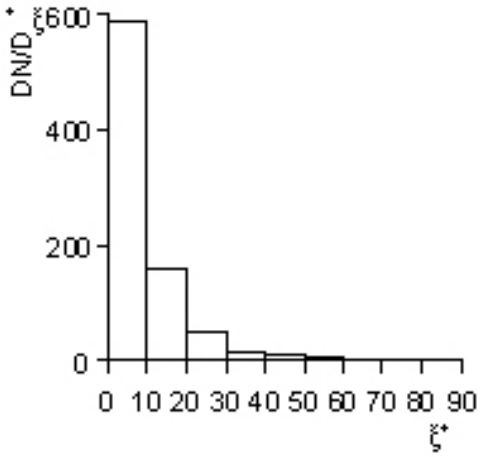


Fig. 7 – The $\xi^+$ angle distribution for central He-Li nuclear collision.

From the angular distribution of peripheral He-Li nuclear collision, we see that most events have $\xi^+ < 10°$. For central He-Li nuclear collision, the $\xi^+$ angular distribution is an equilateral hyperbole, and there are many events that have most probable flow angle greater than 45°. The value of $\xi^+$ angle increases as the contribution of transverse momentum is greater than the contribution of longitudinal momentum for negative pions and there is a conversion of longitudinal into transverse momentum. This conversion of longitudinal into transverse momentum is much stronger in central nuclear collisions than in peripheral nuclear collisions, and at high angles there is a flow of nuclear matter perpendicular to the incident beam direction.

Further analysis of experimental events, depending on the $\xi$ angle values, was performed by defining the two areas according to these values. The two areas were defined according to the $\xi$ angle values, as follows: the "in" area for events that $<\xi^-> \geq \xi \leq <\xi^+>$ and the "out" area for the events that $\xi < <\xi^->$ and $\xi > <\xi^+>$ as shown in Fig. 7.

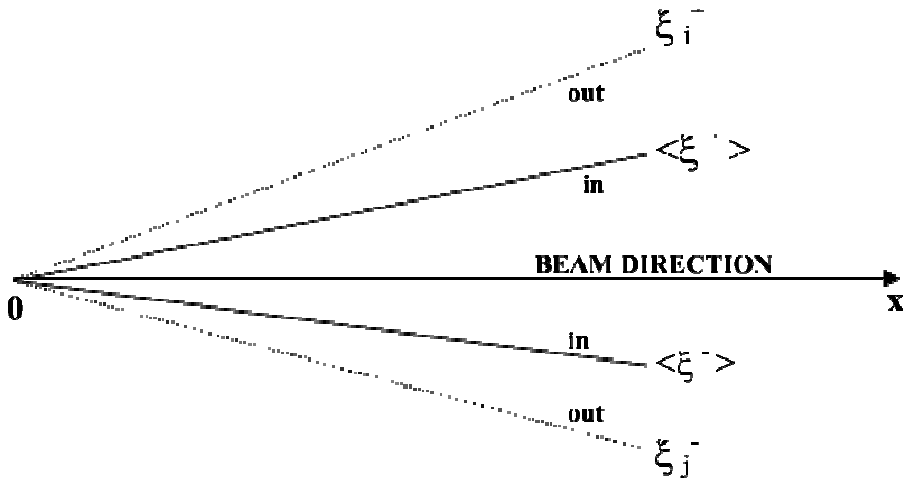


Fig. 8 – Selection of the two areas defined as "in" and "out".

In Table 8 are presented the results for the number of events contained in the two areas, namely: $N_{in}$ – the number of events in the "in" area and $N_{out}$ – the number of events in the "out" area, both for peripheral nuclear collisions, as well as for central nuclear collisions at an incident momentum of 4.5 A GeV/c.

From Table 8, we see that $N_{in}$ is greater than $N_{out}$, independent of the nuclear collision type or trigger mode ($T(0,0)$ is for peripheral collisions, and $T(2.0)$ is for central collisions).

*Table 8*

The number of events contained in the two areas for peripheral nuclear collisions for central nuclear collisions at an incident momentum of 4.5 A GeV/c

| | *T*(0,0) | | | *T*(2,0) | | |
|---|---|---|---|---|---|---|
| $A_P - A_T$ | $N_{ev}$ | $N_{in}$ | $N_{out}$ | $N_{ev}$ | $N_{in}$ | $N_{out}$ |
| He – Li | 2975 | 2017 | 958 | 1129 | 791 | 338 |
| He – C | 1904 | 1429 | 475 | 911 | 629 | 282 |
| He – Ne | 834 | 610 | 224 | 507 | 326 | 181 |
| He – Al | 891 | 698 | 193 | 474 | 343 | 131 |
| He – Cu | 548 | 441 | 107 | 148 | 93 | 55 |
| He – Pb | 395 | 326 | 69 | 173 | 114 | 59 |
| C – C | 490 | 379 | 111 | 245 | 160 | 85 |
| C – Cu | 867 | 638 | 229 | 372 | 260 | 112 |

For the two areas "in" and "out" defined according to the ξ angle values, an analysis of the temperature for the pionic sources and, also, an analysis of the thermalization parameter from these two areas are done.

The temperature of pionic sources was determined using equation (1), namely:

$$< p_T >= c_1 \mathrm{e}^{c_2 \frac{T}{T_0}},$$

where, $T_o$ = 150 MeV, $c_1$ = 382.2 MeV/c and $c_2$ = –0.999.

For thermalization parameter the next relationship has been used:

$$R = \frac{\sum_{j=1}^{n} p_T^j}{\sum_{j=1}^{n} \left| p_L^j \right|}, \tag{10}$$

where $p_T^j$ is the transverse momentum of a negative pion produced in an event, $p_L^j$ is the longitudinal momentum of the same pion.

Determining the pionic source temperature of the two areas is very important to highlight some new states of nuclear matter with high temperatures. The thermalization parameter is an important variable in the dynamic evolution of the nuclear system. With increasing of this parameter occurs also an increase in the nuclear system thermalization degree. Increasing of the thermalization parameter also indicates an increase in the longitudinal momentum conversion in the transverse momentum for negative pions in a nuclear collision. The distribution of thermalization parameter for He-Li central nuclear collision is shown in Fig. 9.

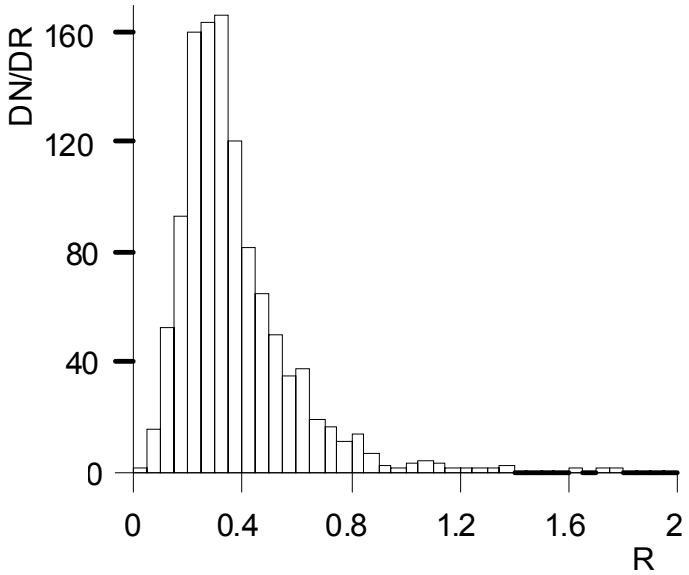


Fig. 9 – The distribution of the thermalization parameter.

It can observe that this distribution may well be fitted with a Poisson distribution, indicating the existence of equilibrium state or a pre-equilibrium state in nuclear matter.

Determination of the pionic source temperatures and the thermalization parameter of the two areas is an analysis made in this work. The obtained results for peripheral and central nuclear collisions at an incident momentum of 4.5 A GeV/c are presented in Table 9 and Table 10. In these tables, $T$ is the temperature of pionic sources, and $R$ is the thermalization parameter for a given collision; $T_{in}$ and $R_{in}$ are the temperature and the thermalization parameter in the "in" area; $T_{out}$ and $R_{out}$ are the temperature and the thermalization parameter in the "out" area.

*Table 9*

The pionic source temperatures and the thermalization parameters for peripheral collisions at an incident momentum of 4.5 A GeV/c

| $A_P - A_T$ | $T$ [MeV] | $T_{in}$ [MeV] | $T_{out}$ [MeV] | $R$ | $R_{in}$ | $R_{out}$ |
|---|---|---|---|---|---|---|
| He – Li | 68.4±0.9 | 78.5±1.1 | 49.1±1.3 | 0.079± 0.001 | 0.066± 0.001 | 0.123± 0.002 |
| He – C | 69.5±0.9 | 76.5±1.1 | 50.2±1.5 | 0.076± 0.001 | 0.064± 0.001 | 0.148± 0.003 |
| He – Ne | 73.3±1.4 | 79.0±1.8 | 58.9±2.3 | 0.087± 0.001 | 0.074± 0.001 | 0.152± 0.006 |
| He – Al | 74.0±1.3 | 80.3±1.6 | 53.4±2.3 | 0.081± 0.001 | 0.069± 0.001 | 0.165± 0.008 |

*Table 9 (continued)*

| | | | | | | |
|---|---|---|---|---|---|---|
| He – Cu | 75.4±1.7 | 80.2±2.0 | 57.1±3.0 | 0.093± 0.003 | 0.079± 0.002 | 0.192± 0.014 |
| He – Pb | 95.6±2.6 | 105.5±2.8 | 56.0±5.2 | 0.077± 0.002 | 0.066± 0.002 | 0.177± 0.017 |
| C – C | 71.3±1.4 | 73.1±1.6 | 65.4±2.7 | 0.144± 0.004 | 0.123± 0.003 | 0.327± 0.021 |
| C – Cu | 80.9±1.5 | 87.0±1.9 | 65.2±2.3 | 0.108± 0.002 | 0.090± 0.002 | 0.204± 0.007 |

From Table 9 we see that:

– $T$, $T_{\text{in}}$ and $T_{\text{out}}$ increase with increasing mass numbers of the target and projectile nuclei;

– $T_{out} < T < T_{in}$ for any nuclear collision;

– $R$, $R_{in}$ and $R_{out}$ increase with increasing mass numbers of the target and projectile nuclei;

– $R_{out} > R > R_{in}$ for any nuclear collision.

*Table 10*

The pionic source temperatures and the thermalization parameters for central collisions at an incident momentum of 4.5 A GeV/c

| $A_P – A_T$ | $T$ [MeV] | $T_{in}$ [MeV] | $T_{out}$ [MeV] | $R$ | $R_{in}$ | $R_{out}$ |
|---|---|---|---|---|---|---|
| He – Li | 99.4±1.2 | 102.1±1.5 | 93.2±1.8 | 0.310± 0.004 | 0.277± 0.004 | 0.420± 0.010 |
| He – C | 100.7±1.1 | 99.7±1.4 | 102.8±2.0 | 0.382± 0.006 | 0.345± 0.006 | 0.508± 0.016 |
| He – Ne | 105.7±1.7 | 106.3±2.2 | 104.6±2.7 | 0.412± 0.009 | 0.364± 0.010 | 0.540± 0.022 |
| He – Al | 106.1±1.5 | 107.4±1.8 | 102.8±2.9 | 0.394± 0.009 | 0.357± 0.008 | 0.539± 0.029 |
| He – Cu | 106.0±4.2 | 111.5±5.8 | 97.1±5.9 | 0.525± 0.028 | 0.433± 0.028 | 0.777± 0.067 |
| He – Pb | 119.0±3.4 | 118.3±4.2 | 120.4±5.7 | 0.474± 0.020 | 0.427± 0.021 | 0.601± 0.049 |
| C – C | 99.8±2.1 | 99.5±2.7 | 100.4±3.4 | 0.375± 0.011 | 0.336± 0.010 | 0.484± 0.029 |
| C – Cu | 111.8±1.9 | 114.6±2.4 | 105.5±3.2 | 0.269± 0.006 | 0.242± 0.006 | 0.357± 0.017 |

From Table 10 we observe that:

– $T$, $T_{in}$ and $T_{out}$ increase with increasing mass numbers of of the target and projectile nuclei;

– $T$, $T_{in}$ and $T_{out}$ do not depend too much of the two areas, the temperatures have similar values;

– $R$, $R_{in}$ and $R_{out}$ increase with increasing mass numbers of of the target and projectile nuclei;

– $R_{out} > R > R_{in}$ for any nuclear collision.

Analyzing the results included in the two tables, it is found that the temperature of the pionic sources is higher for central nuclear collisions than for peripheral nuclear collisions, both for the pionic temperature from each nuclear collision, as well as for the pionic temperature of the two "in" and "out" areas. Also, it is observed that the thermalization parameter is higher in central collisions than in peripheral collisions.

In peripheral nuclear collisions, the temperature in the "out" area decreases in the "in" and the thermalization parameter increases, showing that at large angle $\xi$ values, there is an increase of the thermalization and a decrease of the temperature. The temperature decrease is due to the increase of transverse momentum for negative pions, at large $\xi$ angles there is a conversion of longitudinal momentum in transverse momentum. The increased thermalization shows, also, an increase in transverse momentum of negative pions. For events from the "out" area, it can be assumed the existence of non-equilibrium states and also the possibility of cumulative particle emission.

In central nuclear collisions, the pionic temperature does not depend on the events contained in the two areas, $T_{in} \cong T_{out}$, but the thermalization parameter increases, being higher for the "out" area. The thermalization increase shows that the transverse momentum of negative pions increases for large $\xi$ angles. An increase of thermalization in the "out" area means a decrease of the pionic temperature in this area, but for central collisions this decrease does not occur. This behaviour of the two analyzed parameters show that, if the nuclear collision is central, there is a decrease in longitudinal momentum of negative pions and thus, a strong conversion of longitudinal momentum in transverse momentum for negative pions per event. If the conversion of longitudinal momentum in transverse momentum is strong, there is a flow of nuclear matter perpendicular to the incident beam direction, the flow angle of nuclear matter being greater than 80° [7,18,19].

## 5. FINAL RESULTS AND REMARKS

In this paper an analysis of longitudinal momentum conversion in transverse momentum for nuclear collisions at incident momentum of 4.5 AGeV/c, using the theory presented above, is done. Using equation (9), it was determined the angle between the large ellipse axis (8) and incident beam direction, $\xi$, for several areas of values of longitudinal momentum and transverse momentum for negative pions. The results are presented in Table 11, where $N_\pi$ represents the number of negative pions for each nuclear collision, $p_L$ is the longitudinal momentum, $p_T$ is the transverse momentum, and $p_T^{\max}$ is the maximum transverse momentum of negative pions in a given nuclear collision.

*Table 11*

The behaviour of the ξ angle values for different longitudinal and transverse momenta values

| $A_P - A_T$ | $p_L \in (0, p_T^{max})$ $p_T \in (0, p_T^{max})$ | | $p_L \in (0, p_T^{max}/2)$ $p_T \in (0, p_T^{max})$ | | $p_L \in (0, p_T^{max}/3)$ $p_T \in (0, p_T^{max})$ | |
|---|---|---|---|---|---|---|
| | $N_\pi$ - | ξ [°] | $N_\pi$ - | ξ [°] | $N_\pi$ - | ξ [°] |
| He – Li | 4486 | 20.68±0.01 | 2327 | 73.47±0.04 | 1392 | 84.82±0.02 |
| He – C | 3898 | 27.00±0.03 | 2126 | 75.16±0.03 | 1331 | 83.88±0.02 |
| He – Ne | 2025 | 29.22±0.05 | 1220 | 72.59±0.05 | 846 | 83.36±0.03 |
| He – Al | 1973 | 25.75±0.06 | 1076 | 77.35±0.05 | 689 | 84.26±0.04 |
| He – Cu | 1835 | 32.00±0.09 | 1077 | 77.06±0.05 | 716 | 83.83±0.04 |
| He – Pb | 643 | 32.28±0.27 | 412 | 75.14±0.20 | 284 | 83.55±0.12 |
| C – C | 1317 | 35.33±0.21 | 646 | 77.29±0.07 | 353 | 84.63±0.08 |
| C – Cu | 1243 | 29.24±0.12 | 529 | 83.73±0.11 | 305 | 87.61±0.09 |

From Table 11 we observe that, as the value of longitudinal momentum for negative pions decreases, there is an increase of the ξ angle, the obtained values being greater than 80°. It also highlights a longitudinal momentum conversion in transverse momentum because, as the range of values for longitudinal momentum decreases, the range of values for transverse momentum remains the same. As the contribution of transverse momentum begins to be more important than the contribution of longitudinal momentum for negative pions from a nuclear collision, according to the results in Table 11, there is an increase of the ξ angle (between the large axis of the ellipse (1) and incident beam direction), confirming the flow of nuclear matter perpendicular to the incident beam direction. There is a connection between the ξ angle and the flow angle $\theta_c$ (determined by global analysis).

The main results obtained with the proposed theory presented above are: (i) ellipse (1) from the ($p_L$, $p_T$) plane confirms the ellipsoidal shape of pionic source, obtained both in the global analysis as well as in identical particle interferometry, (ii) can highlight the most probable flow angle of the nuclear matter, making the connection with the "thrust" angle and (iii) can show the flow of nuclear matter perpendicular to the incident beam direction, making the connection with the proposed flow angle in global analysis.

All these results confirm the hydrodynamic behaviour of the nuclear matter formed in the overlapping region of the two colliding nuclei, the influence of the thermalization degree and the collision geometry. The possibility of the formation of some anomal states, as well as the existence of the conditions for phase transitions in hot and dense nuclear matter is confirmed, too. This analysis could help in similar analysis for experimental results obtained in nucleus-nucleus collisions at higher energies, where anomal states and phase transitions are reported, too [23-33].

*Acknowledgments*. We wish Professor Marin IVAŞCU at the 80th anniversary of the birthday many and happy years and address many thanks for the efforts for Romanian Physics development done during the time.

***

The authors are deeply indebted to the collegues from the SKM 200 Collaboration, MARUSYA Collaboration (both at JINR Dubna, Russia), BRAHMS Collaboration (RHIC, BNL, USA) and CBM Collaboration (FAIR, GSI Darmstadt, Germany) for their commom work and help in the data taking and processing.

***

The work of Oana Ristea and Catalin Ristea was supported by the strategic grant POSDRU/89/1.5/S/58852, Project "Postdoctoral programme for training scientific researchers", co-financed by the European Social Found within the Sectorial Operational Program Human Resources Development 2007-2013.

## REFERENCES

1. Călin Beşliu *et al.*, Nucl. Phys., **A672**, 446 (2000).
2. S. Das Gupta, A.Z. Mekjian, Phys. Rep., **72**, 131 (1981).
3. S. Nagamiya, Prog. Part. Nucl. Phys., **XV** 363 (1985).
4. R. Stock, Prog. Part. Nucl. Phys., **XV**, 455 (1985).
5. C. Beşliu, Al. Jipa, Rev. Roum. Phys., **33**, 409 (1988).
6. J.J. Molitoris, D. Hahn, H. Stöcker, Prog. Part. Nucl. Phys., **XV**, 239 (1985).
7. H. Stöcker, W. Greiner, Phys. Rep., **137**, 277 (1986).
8.G.F. Bertsch, S. Das Gupta, **160**, 189 (1988).
9. W. Cassing, V. Metag, U. Mosel, K. Niita, Phys. Rep., **188**, 363 (1990).
10.J. Aichelin, Phys. Rep., **202**, 233 (1991).
11. Al. Jipa, J. Phys. G: Nucl. Part. Phys., **22**, 231 (1996).
12. B.R. Martin, *Statistics for Physicists*, Academic Press, London and New York, 1971.
13. W.T. Eadie *et al.*, *Statistical Methods in Experimental Physics*, North-Holland Publishing Company, Amsterdam, 1971.
14. F. James, Proceedings of the 1970 CERN – Computing and Data Processing School, Via Monastero, Varenna, Italy, 30 August–12 September 1970 - Preprint CERN 71-6 (1971).
15. B. Gndenko, *Theory of probability*, MIR, Moscow,1982.
16. Gh. Mihoc, V. Craiu, *Tratat de Statistică matematică*, Editura Academiei RSR, Bucureşti, 1981.
17. P. Carruthers, C.C. Shih, International Journal of Modern Physics, **A2**, *5*, 1447–1547 (1987).
18. C. Beşliu *et al.*, Rom. Rep. Phys., **48**, *5–6*, 69 (1996).
19. C. Beşliu *et al.*, Eur. Phys.J., **A1**, 65 (1998).
20. G.I. Kopylov, M.J. Podgoretsky, Yad.Fiz., **18**, 656 (1973).
21. C. Beşliu *et al.*, Prog. Part. Nucl. Phys., **XV**, 353 (1985).
22. C. Beşliu, Al. Jipa, Rom. J. Phys., **37**, 1011 (1992).
23. Al. Jipa for the BRAHMS Collaboration, Acta Physica Hungarica A: Heavy Ion Physics, **22**, *1–2*, 121–137 (2005).
24. RHIC BNL Collaborations, Nuclear Physics, **A757**, *1–2*, 1–286 (2005).
25. BRAHMS Collaboration (I. Arsene, I.G. Bearden, D. Beavis, C. Beşliu, ....., Al. Jipa, *et al.*, European Physical Journal, **C43**, 287–293 (2005).
26. BRAHMS Collaboration (I. Arsene, I.G. Bearden, D. Beavis, C. Beşliu, ....., Al. Jipa, *et al.*, Journal of Physics G: Nuclear and Particle Physics, **G31**, *4*, S23–S25 (2005).

27. BRAHMS Collaboration (I. Arsene, I.G. Bearden, D. Beavis, C. Beşliu, ..., Al. Jipa, *et al.*, Phys. Lett., **B650**, 219–223 (2007).
28. BRAHMS Collaboration (I. Arsene, I.G. Bearden, D. Beavis, C. Beşliu, ..., Al. Jipa, *et al.*, Phys. Rev. Lett., **98**, 252001 (2007).
29. Al. Jipa, C. Beşliu, I.S. Zgură, C. Ristea, O. Ristea, A. Horbuniev, I. Arsene, D. Argintaru, M. Călin, T. Eşanu, International Journal of Modern Physics, **E16**, 7–8, 1790–1799 (2007).
30. BRAHMS Collaboration (I. Arsene, I.G. Bearden, D. Beavis, C. Beşliu, ..., Al. Jipa, *et al.*, Phys. Lett., **B677**, 267–271 (2009).
31. C. Beşliu, Al. Jipa, V. Covlea, M. Călin, T. Eşanu, I.V. Grossu, B. Iliescu, C. Bordeianu, A. Scurtu, A. Jinaru, Nucl. Phys., **A820**, 235c–238c (2009).
32. BRAHMS Collaboration (I. Arsene, I.G. Bearden, D. Beavis, C. Beşliu, ..., Al. Jipa, *et al.*, Phys. Lett., **B684**, 22–27 (2010).
33. BRAHMS Collaboration (I. Arsene, I.G. Bearden, D. Beavis, C. Beşliu, ..., Al. Jipa, *et al.*, Phys. Lett., **B687**, 36–41 (2010).